Article

Activity and Recyclability of an Iridium-Edta Water Oxidation Catalyst Immobilized onto Rutile-TiO2

Arianna Savini, Alberto Bucci, Morena Nocchetti, Riccardo Vivani, Hicham Idriss, and Alceo Macchioni

ACS Catal., **Just Accepted Manuscript** • DOI: 10.1021/cs501590k • Publication Date (Web): 25 Nov 2014

Activity and Recyclability of an Iridium-Edta Water Oxidation Catalyst Immobilized onto Rutile-TiO_2

*Arianna Savini,[a] Alberto Bucci,[a] Morena Nocchetti,[b] Riccardo Vivani,[b] Hicham Idriss[c] and Alceo Macchioni[a]**

[a]Department of Chemistry, Biology and Biotechnology, University of Perugia, Via Elce di Sotto 8, I-06123 Perugia, Italy. [b]Department of Pharmaceutical Sciences, University of Perugia, Via del Liceo 1, I-06123 Perugia, Italy. [c]Coroporate Research and Innovation (CRI) centre at SABIC-KAUST, P. O Box 4545-4700, Thuwal 23955, Saudi Arabia.

KEYWORDS: *water oxidation, immobilized catalysts, iridium complexes, rutile-TiO_2, manometry, FEM, TEM, XPS*

ABSTRACT. An iridium heterogenized catalyst for water oxidation (**1**_TiO_2) was synthesized by immobilizing the molecular precursor [Ir(Hedta)Cl]Na (**1**) onto rutile TiO_2. **1**_TiO_2 was evaluated as potential catalyst for water oxidation using CAN (cerium ammonium nitrate) as sacrificial oxidant. **1**_TiO_2 exhibits TOF values between 3.5 min^{-1} and 17.1 min^{-1} and TON > 5000 cycles. Remarkably, TOF of **1**_TiO_2 is almost two times higher than that of the molecular catalytic precursor **1**, under very similar experimental conditions. The reusability of **1**_TiO_2 is also remarkable. As a matter of fact, it remains active after ten catalytic runs. Despite **1**_TiO_2 was tested under necessarily oxidative and acidic (pH 1, 0.1 M HNO_3) experimental conditions,

it proved to be capable of completing more than 5000 cycles with a constant TOF = 12.8 min^{-1}, when a single addition of CAN is used. Some leaching of iridium from **1**_TiO_2 was observed only after the first catalytic run leading to **1'**_TiO_2. **1**_TiO_2 and **1'**_TiO_2 were characterized by several analytical techniques. It was found that iridium atoms are uniformly dispersed on both **1**_TiO_2 and **1'**_TiO_2 samples. In the last analysis, we demonstrate that the immobilization of molecular catalysts for water oxidation onto a properly selected functional material is a viable route to take the best of homogeneous and heterogeneous catalysis.

1. INTRODUCTION

It is now evident that both the reductive generation of solar fuels, through an artificial photosynthetic process, and the production of electric energy, *via* a photo-electrochemical cell, strongly rely on electrons derived from water oxidation to molecular oxygen.[1-6] As a consequence, it is not surprising that considerable efforts are directed toward the development of new and better performing heterogeneous[7-10] and homogeneous[11-22] water oxidation catalysts.[23] Heterogeneous catalysts are easier to integrate in a practical apparatus and are usually more robust than homogeneous catalysts, which may transform[24] through associative processes under the harsh conditions used in catalysis. On the other hand, homogeneous catalysts can be rationally designed through the selection of the ancillary ligands, possibly guided by the knowledge of the reaction mechanism. The immobilization of a molecular catalyst onto a surface of a properly selected functional material, thus obtaining a heterogenized catalyst, has been proposed as a procedure to take the best of both worlds.[25-30] In this respect, TiO_2 is the material of choice for redox applications due to its high photocatalytic properties, low cost, stability and

nontoxicity.[31-34] Nevertheless, only in a few cases molecular catalysts for water oxidation have been successfully supported onto TiO_2.[28,35-37]

Over the last few years, after the seminal papers by Bernhard[38] and Crabtree,[39] we[40-44] and others[45-54] have been involved in the synthesis of novel iridium-based molecular catalysts for water oxidation that exhibited remarkable performances. Particularly, we focused some of our attention on molecular catalysts having a pendant functionality suitable to be anchored onto a solid support.[42,43] Perhaps, the most intriguing of them is [Ir(Hedta)Cl]Na (Hedta = monoprotonated ethylene-diaminetetraacetic acid) (**1**, Scheme 1) due to the simplicity of its preparation, high solubility in water and the natural presence of a peripheral pendant –COOH functionality suitable for immobilization on a solid support.[42] In particular the –COOH group is suitable to interact with the dominant orientation (110) of the rutile TiO_2 surface, where the Ti…Ti distance of 3 Å allows for a stable bridging configuration as seen by numerous studies including Scanning Tunnelling Microscopy (STM),[55-57] Electron-Stimulated Desorption Ion Angle Distribution (ESDIAD)/Low Energy Electron Diffraction (LEED),[58] IR,[59] Near edge X-ray absorption fine structure (NEXAFS),[60] X-ray Photoelectron Diffraction (XPD)[61,62] and Density Functional Theory (DFT) computation.[63-65] In homogeneous phase **1** (0.5-7 μM) showed a TOF of ca. 7 min^{-1} and a remarkably high TON for the catalytic oxidation of water driven by CAN (cerium ammonium nitrate).[42]

Herein we show that **1** can be successfully immobilized onto rutile-TiO_2 leading to a heterogenized catalyst (**1**_TiO_2, Scheme 1) exhibiting higher TOF than **1** in water oxidation driven by CAN. Furthermore, **1**_TiO_2 can be reused several times with only a marginal decrease of activity. **1**_TiO_2, as well as the material obtained after the first catalytic run (**1'**_TiO_2), were characterized by powder X-ray diffraction analysis (PXRD), inductively coupled plasma-optical

emission spectrometry (ICP-OES), transmission electron microscopy (TEM), field emission scanning electron microscopy (FE-SEM), elemental mapping performed by X-ray spectroscopy (EDS) supported by FE-SEM and X-ray photoelectron spectroscopy (XPS).

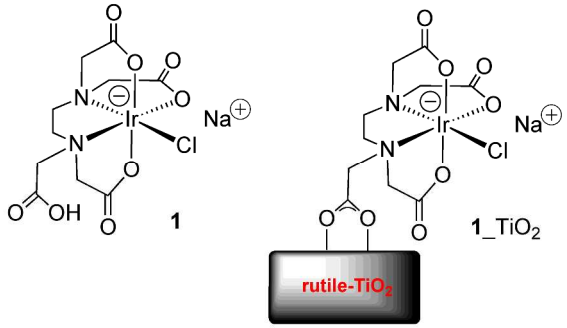

Scheme 1. Sketch of the molecular and heterogenized water oxidation catalysts **1** and **1**_TiO_2, respectively.

2. RESULTS AND DISCUSSION

1_TiO_2 was prepared by dispersing nanoparticles of rutile-TiO_2 in a water solution of **1** at 25°C (Experimental Section). **1**_TiO_2 was recovered by centrifugation and washed several times with water, 0.1 M HNO_3 water solution, acetonitrile and dichloromethane, and finally, dried under *vacuum*. ICP-OES analysis (Experimental Section) indicated 0.059% w/w of iridium loading in **1**_TiO_2, corresponding to a concentration of the iridium complex of 3.1 μmol g^{-1}.

Activity of **1**_TiO_2 in water oxidation was checked by using Ce^{4+} (added as CAN) as a sacrificial oxidant, dispersing the proper amount of catalyst in acidic water (pH 1, 0.1 M HNO_3) at 25°C.

$$4Ce^{4+} + 2H_2O \rightarrow 4Ce^{3+} + 4H^+ + O_2 \quad (1)$$

The evolved gas, according to equation 1, was quantified by differential manometry (Experimental Section).[66]

In a first series of experiments 261, 771 and 1295 equivalents of CAN with respect to the iridium were added to suspensions of about 62 mg of **1**_TiO_2, in a total volume of 5.5 mL of acidic water (pH 1, 0.1 M HNO_3) (Table 1). Oxygen evolution was observed in all cases until complete consumption of CAN (Table 1).[67] Derived TOF values were found to increase with increasing CAN concentration from 3.5 min^{-1} up to 17.1 min^{-1} (Table 1, entries 1, 7 and 14), as often observed also for homogeneous catalysts.[31,35,36,68,69] In order to evaluate its reusability, **1**_TiO_2 was recovered by centrifugation and washed with acidic water; its activity and that of the supernatant solution were tested by using the same amount of CAN of the previous experiment. Data are reported in Table 1 and Figure 1. As it can be seen from Table 1, the recovered solid maintains most of its activity when reused. Also the first supernatant solution is active in water oxidation but, interestingly, the catalytic profile is rather different from that of solid materials. This is clearly shown in Figure 1, where it is possible to appreciate that **1**_TiO_2 has the typical gas evolution *versus* t trend in which, after a short induction time, there is a linear increase of the amount of evolved gas until a plateau is reached. **1'**_TiO_2 exhibits an analogous TON *versus t* trend just a minor decrease in the slope and a much smaller (if any) induction time. On the contrary, the first supernatant solution shows a sigmoidal trend (Figure 1) indicating an increase of activity at the end of the catalytic process. The second supernatant is not active at all (Figure 1). It can be supposed that some iridium catalytic centres, more weakly bound to the solid support in **1**_TiO_2, leach out during the first catalytic run. The content of iridium in **1'**_TiO_2 was evaluated by ICP-OES. It was found that about 30.0% of the iridium of **1**_TiO_2 is released into solution during the reaction with CAN and thus the calculated iridium loading in **1'**_TiO_2 is 2.2 μmol g^{-1}. This allowed also the concentration of iridium in the supernatant to be derived (Table 1). Consequently, TOF of the supernatant solution, calculated in the last part of TON *versus* t

trends, where the slope is maximum, is in the 6.9 min^{-1} – 14.3 min^{-1} range (Table 1, entries 2, 8 and 15). The catalytic activity of the recovered solid drops by 13-56% after each run (Table 1) and the decrease seems to be higher when a higher concentration of CAN is used (compare entries 1, 3, 5, 6 with entries 7, 9, 11, 13 and entries 14, 16, 18 in Table 1). Suspecting that at least part of this drop could be due to some loss of catalyst during the centrifugation and, especially, washing procedures, we repeated the experiment with 62 mg of **1**_TiO_2 and 250 μmol of CAN, thus reproducing the same conditions of the experiment whose results are reported in entries 14-18 of Table 1, separating the supernatant and washing the solid only after the first catalytic run. Successive runs were performed by adding fresh aliquots of CAN, after centrifugation and removal of supernatant, without washing the powder (entries 19-23 in Table 1). Results clearly indicate a much smaller drop of activity (compare entries 14, 16, 18 with entries 19, 20, 21 in Table 1).

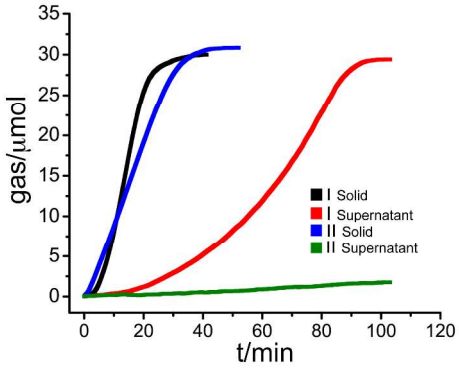

Figure 1. First two catalytic runs performed by the addition of around 150 μmol of CAN (0.5 mL) to a suspension of 62.1 mg of **1**_TiO_2 in 5.0 mL of water at pH 1 (by HNO_3). Activity of supernatant solutions was also tested by adding the same amount of CAN used in the runs with the solid.

Table 1. Multiple catalytic runs performed with **1**_TiO_2 by adding three different amounts of CAN.

Entry	Run	C_{Ir} [μM]	C_{CAN} [mM]	C_{CAN}/C_{Ir}	$k_{obs}\cdot10^9$ [mol s^{-1}][a]	TOF [min^{-1}][b]	TON[c]	O_2 yield
1	I_{solid}	35.2[d]	**9.2**	**261**	11.2	**3.5**	46	70%
2	$I_{supernatant}$	9.5[e]	9.1	958	6.7[f]	6.9	141	59%
3	II_{solid}	24.6[g]	9.2	374	9.6	4.2	78	83%
4	$II_{supernatant}$	~0	9.9	n.a.	~0	n.a.	0	0%
5	III_{solid}	24.6[g]	9.3	378	8.2	3.6	77	81%
6	IV_{solid}	24.6[g]	9.3	378	5.9	2.6	72	76%
7	I_{solid}	35.0[d]	**27.0**	**771**	32.3	**10.1**	156	81%
8	$I_{supernatant}$	9.5[e]	30.0	3158	10.8[f]	13.7	622	79%
9	II_{solid}	24.5[g]	27.0	1102	16.9	7.5	228	83%
10	$II_{supernatant}$	~0	28.6	n.a.	~0	n.a.	0	0%
11	III_{solid}	24.5[g]	27.0	1102	13.5	6.0	214	78%
12	$III_{supernatant}$	~0	28.6	n.a.	~0	n.a.	0	0%
13	IV_{solid}	24.5[g]	27.0	1102	11.8	5.2	221	80%
14	I_{solid}	35.2[d]	**45.6**	**1295**	55.1	**17.1**	280	86%
15	$I_{supernatant}$	9.5[e]	50.0	5263	11.4[f]	14.3	1076	82%
16	II_{solid}	24.6[g]	45.6	1854	25.6	11.3	353	76%
17	$II_{supernatant}$	~0	48.2	n.a.	~0	n.a.	0	0%
18	III_{solid}	24.6[g]	45.7	1858	14.2	6.3	357	77%
19	I_{solid}	35.1[d]	45.7	1302	57.2	17.8	249	77%
20	II_{solid}	24.6[g]	45.6	1854	31.0	13.8	349	75%
21	III_{solid}	24.6[g]	45.7	1858	26.3	11.7	421	91%
22	IV_{solid}	24.6[g]	45.7	1858	20.0	8.9	412	89%
23	V_{solid}	24.6[g]	45.6	1854	15.1	6.7	407	88%

[a]From gas production (mol) *vs.* time (s) linear trend in the initial part of the reaction; [b]from (k_{obs}/mol_{Ir})·60; [c]from total gas produced (μmol)/cat(μmol); [d]based on a catalyst loading of 3.1 μmol g^{-1} in **1**_TiO_2 calculated from ICP-OES data; [e]based on the fact that ICP-OES analysis indicated that 30.0% of the initial content of catalyst in **1**_TiO_2 is released into solution during the first catalytic run (I_{solid}); [f]from gas production (mol) *vs.* time (s) in the last part of the reaction, corrected for dilution factors in order to better compare with values obtained in the runs with the solid; [g]based on a catalyst loading of 2.2 μmol g^{-1} (70.0% of the initial value based on ICP-OES data).

2.1 Catalytic water oxidation with 1'_TiO_2

Having realized that the material recovered after the first catalytic run (**1'**_TiO_2) does not undergo further leaching, we decided to prepare **1'**_TiO_2 in large quantity, as described in Experimental Section, and evaluate its catalytic performance, in terms of TOF, TON and reusability, more in detail.

At this aim, multiple aliquots of 100 μL of CAN (50 μmol) were repeatedly added to suspensions of about 56, 28 and 13 mg of **1'**_TiO_2, respectively, in 5 mL of acidic water (pH 1, 0.1 M HNO_3) (Table 2). Since **1'**_TiO_2 material contained 2.2 μmol g^{-1} of iridium catalyst (see above), in the three experiments reported in Table 2 about 420, 820 and 1800 equivalents of CAN, respectively, were added in each consecutive addition.

As found before (Table 1), TOF values increase with increasing C_{CAN}/C_{Ir} ratio value (Figure 2). In particular, in the first experiment, in which C_{CAN}/C_{Ir} = 412 a TOF value of 9.1 min^{-1} was measured (Table 2, entry 1), whereas in the second and in the third experiments, in which C_{CAN}/C_{Ir} was, respectively, equal to 833 and 1754, TOF values were 15.1 and 16.6 min^{-1} (Table 2, entries 11 and 19).

A drop of activity was observed in the three experiments after each catalytic run (Table 2): TOF values decreased from 9.1 to 2.8 min^{-1} moving from the first to the tenth catalytic run with 420 equivalents of CAN (Table 2, entries 1-10); over 8 catalytic runs of 820 equivalents of CAN each one, TOF values decreased from 15.1 to 4.4 min^{-1} (Table 2, entries 11-18 and Figure 2); and, finally, in the last experiment reported in Table 2 (entries 19-24), after 6 consecutive additions of around 1800 equivalents of CAN, TOF values dropped from 16.6 to 5.4 min^{-1}.

Catalyst deactivation seems to be more evident when many additions of a small amount of CAN are performed. For example after around 700 catalytic cycles, in the first experiment

reported in Table 2 TOF value (entry 10) corresponds to a 31% of the initial value (entry 1), while in the second experiment (entry 14) it is 43% of it (entry 11), and in the last (entry 20) it corresponds to 60% of the initial TOF value (entry 19). Notably, in this last experiment, **1'**_TiO_2 is still active with a TOF of 5.4 min^{-1} after a total of 1953 catalytic cycles (Table 2, entry 24).

A direct comparison between the catalytic activity of immobilized **1'**_TiO_2 and homogeneous **1** was performed, carrying out a multiple run experiment also for **1** under experimental conditions as more as possible similar to those used for **1'**_TiO_2 (see TOF values in parentheses of entries 1-10 in Table 2 and Figure 3). TOF values for **1'**_TiO_2 decrease from 9.1 min^{-1} (run 1) to 2.8 min^{-1} (run 10). Those of **1** are almost two times lower and pass from 5.9 min^{-1} (run 1), a value perfectly consistent with what previously reported by us,[42] down to 1.5 min^{-1} (run 10) (Table 2). On the other hand, the two catalytic systems exhibit comparable TON values. It is interesting to outline that all catalytic runs with **1'**_TiO_2 do not show any induction period, whereas some increase of activity is observed in the first 2-3 catalytic runs with **1** (Figure 3).

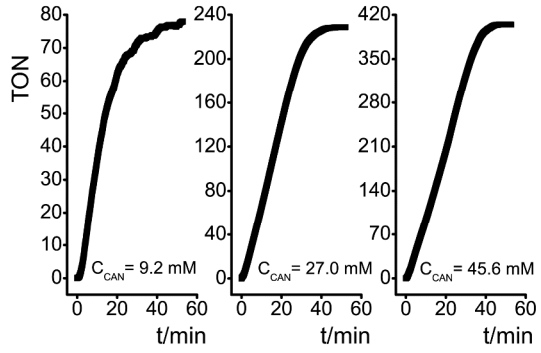

Figure 2. TON *versus* time trends for catalytic experiments carried out by II_{solid} (C_{Ir}=24.5-24.6 μM, pH 1, 0.1 M HNO_3) at different concentration of CAN (data are reported in Table 1, entries 3, 9 and 16).

The pronounced decrease of activity observed when more CAN additions were performed at the same total number of equivalents seems to indicate that **1'**_TiO_2 could exhibit better performances when a single addition of a large excess of CAN is used. This was just the case. When a single aliquot of 46915 equivalents of CAN was added to a suspension of **1'**_TiO_2 a TON of 6596 was measured after around 16 hours and, notably, a constant TOF of 12.8 min^{-1} was observed for more than 6 h (>5000 catalytic cycles) (ESI). The latter catalytic performances are outstanding.

Table 2. Three experiments in which multiple catalytic aliquots of around 50 μmol of CAN (100 μL) were added to different amounts of **1'**_TiO_2 dispersed in 5 mL of acidic water (pH 1, 0.1 M HNO_3).

Entry	Run	C_{Ir} [μM][b]	C_{CAN} [mM]	C_{CAN}/C_{Ir}	TOF[a] [min^{-1}][c]	Total cycles[d]
1	I	**24.3 (25.0)**	10.0	**412**	**9.1 (5.9)**	77
2	II	23.8 (24.4)	9.9	416	7.0 (4.5)	155
3	III	23.3 (23.8)	9.7	416	5.5 (3.4)	227
4	IV	22.9 (23.3)	9.5	415	5.3 (2.4)	309
5	V	22.5 (22.7)	9.3	413	5.2 (2.2)	391
6	VI	22.1 (22.2)	9.2	416	4.1 (1.9)	456
7	VII	21.7 (21.7)	9.0	415	3.8 (1.8)	534
8	VIII	21.3 (21.3)	8.9	418	3.3 (1.7)	605
9	IX	21.0 (20.8)	8.7	414	3.0 (1.6)	675
10	X	20.6 (20.4)	8.6	417	2.8 (1.5)	746
11	I	**12.0**	10.0	**833**	**15.1**	166
12	II	11.8	9.4	797	9.2	317
13	III	11.6	9.8	819	7.5	489
14	IV	11.4	9.6	842	6.5	653
15	V	11.2	9.4	839	5.8	801
16	VI	11.0	9.0	818	5.3	954
17	VII	10.8	8.9	824	4.8	1110
18	VIII	10.6	8.7	821	4.4	1263
19	I	**5.7**	10.0	**1754**	**16.6**	333
20	II	5.6	9.8	1750	9.9	714
21	III	5.5	9.6	1745	8.1	1033
22	IV	5.4	9.5	1759	6.2	1304
23	V	5.3	9.3	1755	5.9	1644
24	VI	5.2	9.1	1750	5.4	1953

[a]TOF values in parentheses refer to a multiple run experiment carried out using **1** as homogeneous catalyst (C_{Ir} = 25 μM, C_{CAN} = 10 mM); [b]based on a catalyst loading of 2.2 μmol g^{-1} (70.0% of the initial value based on ICP-OES data); [c]from (k_{obs}/mol_{Ir})·60 (where k_{obs} is derived from gas(mol) produced *vs.* time(s) linear trend in the first part of the reaction, corrected for dilution factors); [d]cumulative catalytic cycles performed in each run.

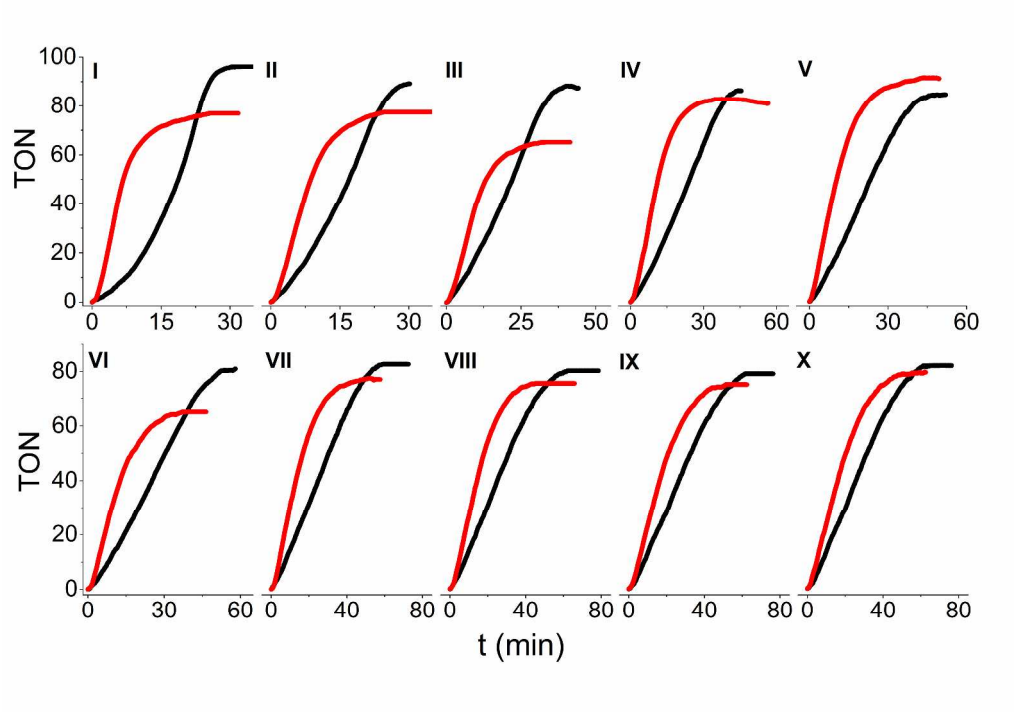

Figure 3. TON *versus* time trends for two multiple run experiments carried out for **1'**_TiO_2 (red) and **1** (black) under very similar experimental conditions (entries 1-10, Table 2).

2.2 Structural and morphological characterization of 1_TiO_2 and 1'_TiO_2

The PXRD patterns of **1**_TiO_2 and **1'**_TiO_2 (Figure 4) are identical; as it is usually the case when small amounts of metals are deposited on a crystalline support. They show that no other diffraction peaks except those belonging to the rutile substrate phase emerged after functionalization and after the first catalytic run. Furthermore, no additional line broadening is observed in the pattern after the catalytic run, assessing that also microstructural parameters (crystallite size and lattice defects) are similar for the two samples.

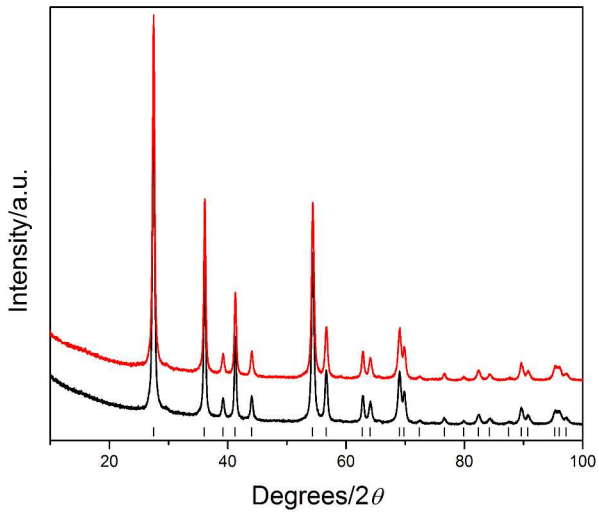

Figure 4. X-ray powder diffraction patterns of **1**_TiO_2 (black line) and **1'**_TiO_2 (red line). Black marks indicate the calculated positions of rutile peaks.

These observations were confirmed by FE-SEM and TEM analysis. TEM micrographs of the pristine TiO_2 and the two samples did not show relevant differences. As an example Figure 5 shows a TEM image of **1'**_TiO_2. All of these images show samples made of prismatic crystallites with dimensions of about 30 nm x 100 nm (+/- 10 nm), and no highly contrasted structures, that might be ascribed to heavy iridium phases, were observed.

Elemental mappings of Ir and Cl in **1**_TiO_2 and **1'**_TiO_2 samples were obtained by the FE-SEM-EDS technique (Figure S10, Supporting Information). In these images, the local concentration of one element is indicated by the brightness and the intensity of the black spots. From these data we can assess that iridium atoms are uniformly distributed throughout the particles of the two samples. They also show that distribution of Cl nicely tracks that of Ir in both **1**_TiO_2 and **1'**_TiO_2. The comparison between iridium and chlorine maps taken before and after a catalytic run, seems to confirm, although qualitatively, the reduction of immobilized catalyst content indicated by ICP data.

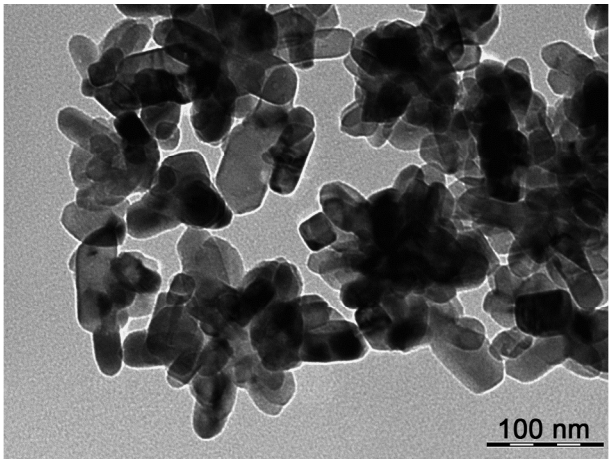

Figure 5. TEM image of **1'**_TiO_2. Scale bar corresponds to 100 nm.

In summary, combining PXRD and electron microscopy data, it is possible to state that iridium atoms are uniformly dispersed on the samples before and after the catalytic run, and do not form separate aggregates larger than a few nanometers.

2.3 XPS spectroscopy studies

X-ray photoelectron spectroscopy was conducted on **1**_TiO_2 in order to extract quantitative information on the surface composition of the catalyst. The overlap between the Ti3s and $Ir4f_{7/2}$ makes it difficult to accurately compute for the amount of Ir on the surface as well as to investigate its chemical state. However, because the $Ir4f_{5/2}$ line is above that of Ti3s it is possible to recalculate the amount of $Ir4f_{7/2}$ and deduct it from the overall peak seen at the Ti3s/$Ir4f_{7/2}$ position. Figure 6 presents the Ti3s region in which a fitting for the $Ir4f_{5/2}$ at a BE = 64.4 eV was made. Based on the splitting between the $Ir4f_{7/2,5/2}$ of 3.0 eV[70,71] a peak at 61.3 eV was generated with the theoretical contribution of 4/3 times that of $Ir4f_{5/2}$. In order to further confirm the Ir presence we sought the Ir4d region; typically 3-5 times weaker than that of Ir4f. The inset in the Figure 6 presents the Ir4d region, which lies just above the C1s region making

the background high, which further affects the signal to noise ratio. The presence of the two peaks with a splitting of 15.0 eV can be another evidence for Ir. Therefore we have curve fitted for the two main peaks at 297.0 and 312.0 eV attributed to $Ir4d_{5/2}$ and $Ir4d_{3/2}$ respectively (BE position are with +/- 0.2 eV due to the weak signal to noise ratio). Other peaks above each line are however present by ca. 5 and 9 eV. The large separation of these two peaks from the parent ones rules out possible attribution to changes in the chemical environment of the Ir atoms. These can be tentatively attributed to shake up satellites. Detailed satellite structures of Ir4d are however not available to further validate their attributions. In order to further probe into the Ir signal we have opted to Ar-ions sputtering of the surface. Ion sputtering does affect the surface in several ways in addition to cleaning it from adventitious contaminants. It reduces the heavy elements due to preferential removal of oxygen atoms (leaving behind electrons).[72] In the process however some Ir may have been sputtered away too as a result of breaking the Ir-O and Ir-N bonds. Supporting Information presents the Ir4d region upon Ar ions sputtering. While the signal to noise has further decreased because of the rise of the base line due to some Ar ions that are implanted on the surface (Ar2s lines are at about 319.5 eV) the Ir signal still persists albeit slightly smaller.

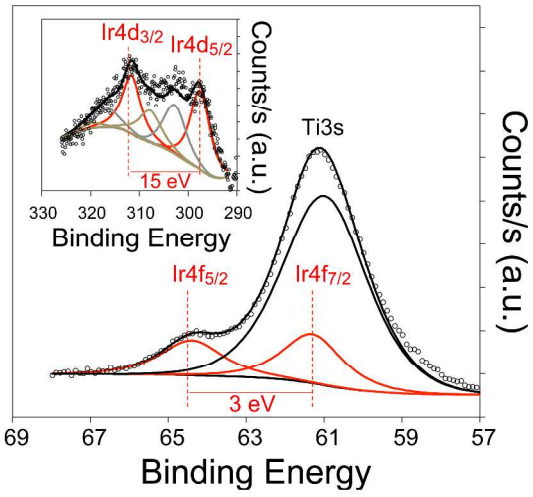

Figure 6. XPS Ti3s/Ir4f of **1**_TiO_2 before reaction. Inset: XPS Ir4d region. Spin splitting is indicated by ΔE.

In summary the presence of $Ir4f_{5/2}$, and Ir4d in the fresh sample and the persistence of the signal of the Ir4d in the sputtered surface give confidence that indeed Ir complexes have been deposited on the surface of TiO_2 and are responsible for the enhancement of the oxygen evolution reaction. Table 3 gives the computed peak areas. Based on the 4f lines Ir represents about 0.6 at. % of the surface (neglecting satellites contributions) with an Ir/Ti ratio of about 0.02.

Table 3. Quantitative analysis of **1**_TiO_2 using XPS based on both the Ir4d and Ir4f.

	Ir/Ti atomic	Ir atomic%
Based on Ir4d (with satellites)	0.037	1.10
Based on Ir4d (without satellites)	0.020	0.70
Based on Ir4f	0.018	0.60

3. CONCLUSIONS

We demonstrated that the immobilization of a molecular catalyst onto the surface of a properly selected functional material is a very promising strategy to develop efficient catalysts for water oxidation. As a matter of fact, the previously reported molecular catalyst [Ir(Hedta)Cl]Na (**1**)[42] improves its performance toward water oxidation when immobilised onto rutile TiO_2. All techniques exploited to characterize the immobilized catalyst, before (**1**_TiO_2) and after (**1'**_TiO_2) the first catalytic run, indicated that iridium is uniformly dispersed on the samples thus excluding the formation of domains of aggregation, at least with nanometric dimensions.

The results reported in this paper are extremely encouraging for future applications of this material, and analogous ones, in the photocatalytic water oxidation. Experiments in such a direction are in progress in our laboratories.

4. EXPERIMENTAL SECTION

Complex **1** was synthesized by the reaction of $IrCl_3.nH_2O$ with Na_2H_2edta according to a literature procedure.[73]

Preparation of 1_TiO_2. A solution of complex 1 (3.9-7.7 mg) in milliQ water (ca. 2 mL) was added to rutile-TiO_2 nanoparticles (0.8-1.7 g) dispersed in water (ca. 5 mL) at 25°C. The mixture was kept under stirring for a few hours and, afterward, the solid was recovered by centrifugation and washed several times with water, a solution 0.1 M of HNO_3 in water, acetonitrile and dichloromethane, and finally, dried under *vacuum*.

Preparation of 1'_TiO_2. 300 mg of **1**_TiO_2 were reacted with 0.242 mmol of CAN in a total volume of 5.5 mL of water at pH 1 (by HNO_3) at 25°C. Water oxidation reaction was monitored by manometry (see below) and when the gas production was finished, the mixture was

centrifuged. The supernatant solution was collected for elemental analysis and the solid was recovered, washed two times with a 0.1 M solution of HNO_3 in water and three times with milliQ water. Finally, the solvent was removed by evaporation under reduced pressure and the solid **1'**_TiO_2 was dried under *vacuum.*

Water oxidation experiments. Water oxidation experiments were performed at pH 1 (by HNO_3) using CAN as the sacrificial oxidant. Gas production was monitored through manometric measurements performed with homemade water-jacket glass tubes coupled to a Testo 521-1 manometer.

In a first series of experiments, a **1**_TiO_2 sample (62.1-62.4 mg) was transferred in a homemade glass tube (working cell) equipped with a side arm for the connection with the manometer and with a septum for the injection of the oxidant solution. A stir bar was placed inside the tube and 5 mL of water at pH 1 (by HNO_3) was added to the solid. The same amount of solvent was transferred into another identical glass tube (reference cell). Both tubes were closed with a septum and connected to the manometer. The system was kept at a constant temperature of 25°C and allowed to equilibrate with stirring for at least 20 min. When a steady baseline was achieved, the solvent solution (0.5 mL) was added into the reference cell, and the oxidant solution (0.5 mL, 0.051-0.251 mmol) was added into the working cell. Gas evolution was monitored during the reaction by measuring the differential pressure between the two cells.

Once the gas production was finished (as the sacrificial oxidant was all consumed) the mixture into the working cell was centrifuged. 4.5-4.7 mL of the supernatant solution was recovered and tested in water oxidation by the addition of the same amount of CAN used for the previous reaction. The remained solid was washed two times with acidic water (pH 1, 0.1 M HNO_3) and reused for several catalytic runs performed under exactly the same conditions. After

each catalytic run, the solid was centrifuged and washed 2-3 times with acidic water. In some cases the activity of recovered supernatant solutions was tested.

Rate constant k_{obs} (mol s^{-1}) was derived from gas evolution (mol) *versus* time (s) linear trends in the first part of the reaction. k_{obs} values derived for the experiments carried out with supernatant solutions were corrected for dilution factors in order to better compare their values with the ones observed in the reaction with the solid. Entries 19-23 of Table 1 refer to an experiment in which the solid was washed only after the first catalytic run and reused in subsequent catalytic runs after centrifugation, removal of the supernatant and addition of fresh acidic solution. TOF (min^{-1}) values were calculated from $(k_{obs}/mol_{Ir})\cdot 60$, where mol_{Ir} is the amount of iridium contained in the solid material or in supernatant solutions used in the reactions, based on ICP-OES data. All results obtained in these experiments are summarized in Table 1.

In another series of experiments a **1'**_TiO_2 sample (13.245-56.245 mg) was transferred into the working cell and 5.0 mL of acidic water (pH 1, 0.1 M HNO_3) was added to the solid. The same amount of solvent was transferred into the reference cell and both tubes were kept at a constant temperature of 25°C, connected to the manometer and allowed to equilibrate with stirring for at least 20 min. When a steady baseline was achieved, the solvent solution (100 μL) was added into the reference cell, and the oxidant solution (100 μL, 0.051-0.052 mmol) was added into the working cell. Gas evolution was monitored by manometry and, once the gas production stopped, both the tubes were disconnected from the manometer. The system was allowed to re-equilibrate at atmospheric pressure and, then it was reconnected to the manometer for another catalytic run that was carried out as the previous one. This procedure was repeated 6-10 times. k_{obs} values were derived from gas evolution (mol) *versus* time (s) linear trends in the

first part of the reaction and corrected for dilution factors. TOF (min^{-1}) values were calculated from (k_{obs}/mol_{Ir})·60, where mol_{Ir} is the amount of iridium contained in the solid material used in the reactions, based on ICP-OES data. All results obtained in these experiments are collected in Table 2.

Finally, the maximum number of catalytic cycles (TON) that catalyst **1'**_TiO_2 can undergo were determined in a manometric experiment in which 1.45 mL of the oxidant solution (1.092 mmol) were added to a suspension of 10.580 mg of **1'**_TiO_2 in 0.5 mL of acidic water (pH 1, 0.1 M HNO_3) (see ESI).

A maximum *a priori* error of ca 20% in TON and TOF was estimated by considering the uncertainty of weighting, preparation of catalyst and CAN solutions, CAN injection, instrumental precision, standard deviation of TON *versus* t trends (only for TOF).

Instrumental Measurements. PXRD patterns were taken with a Philips X'PERT PRO MPD diffractometer operating at 40 kV and 40 mA, with a step size 0.017° 2θ, and step scan 150 s, using Cu Kα radiation and an X'Celerator fast detector.

The morphology of the samples was investigated with a Philips 208 transmission electron microscope and with a FEG LEO 1525, scanning electron microscope. This latter instrument supported an energy dispersive X-ray spectrometer for elemental Ir mapping.

FE-SEM micrographs were collected after depositing the samples on a stub and sputter coating with chromium for 20 s.

Metal analysis were performed with Varian 700-ES series inductively coupled plasma-optical emission spectrometers (ICP-OES). A concentrated stock solution of iridium was prepared by dissolving dried $IrCl_3$ in concentrated HCl until reaching a volume of 1 L of

solution. Working calibration solutions were prepared from the stock solution by making 300-, 100-, 60- and 30- fold dilutions.

For the analysis of **1**_TiO_2, a weighed amount of the solid (about 180 mg) and around 500 mg of $(NH_4)_2SO_4$ were dissolved in *ca.* 40 mL of H_2SO_4 under reflux at T ~ 350°C. The solution was allowed to cool at room temperature and then brought to a final volume of 50 mL by the addition of milliQ water. A diluted solution (1:2) was used for ICP analysis and the iridium content was determined by ICP-OES.

The supernatant solution collected after a catalytic run during the procedure followed for the preparation of **1'**_TiO_2 (see text above) was directly analyzed by ICP-OES for determining the amount of iridium released during catalysis.

X-Ray Photoelectron Spectroscopy was conducted using a Thermoscientific ESCALAB 250 Xi, equipped with a mono-chromated AlKα X-ray source, Ultra Violet He lamp for UPS, ion scattering spectroscopy (ISS), and reflected electron energy loss spectroscopy (REELS) was used. The base pressure of the chamber was typically in the low 10^{-10} mbar range. Charge neutralization was used for all samples (compensating shifts of ~1 eV). Spectra were calibrated with respect to C1s at 284.7 eV. The Ti3s/Ir4f, Ti2p, O1s, Ir4d were scanned for both the fresh and used catalysts. Typical acquisition conditions were as follows: pass energy = 20 eV and scan rate = 0.1 eV per 200ms. Ar ion bombardment was performed with an EX06 ion gun at 1 kV beam energy and 10 mA emission current; sample current was typically 0.9-1.0 μA. The sputtered area of 900 x 900 μm^2 was larger than the analyzed area: 600 x 600 μm^2. Self-supported oxide disks of approximately 0.5 cm diameter were loaded into the chamber for analysis. Data acquisition and treatment was done using the Avantage software.

SUPPORTING INFORMATION. Additional figures on catalytic experiments and analytical characterization of immobilized catalysts. This material is available free of charge via the Internet at http://pubs.acs.org.

AUTHOR INFORMATION

Corresponding Author

Email: alceo.macchioni@unipg.it, fax +39 075 5855598, phone +39 075 5855579

ACKNOWLEDGMENT. We thanks SABIC and Regione Umbria (POR FSE Projects) for financial support.

REFERENCES

(1) Lewis, N. S.; Nocera, D.G. *Proc. Natl. Acad. Sci. U.S.A.* **2006**, *103*, 15729-15735.

(2) Balzani, V.;Credi, A.; Venturi, M. *ChemSusChem* **2008**, *1*, 26-58.

(3) Gust, D.; Moore, T. A.; Moore, A. L. *Acc. Chem. Res.* **2009**, *42* (12), 1890-1898.

(4) Alstrum-Acevedo, J. H.; Brennaman, M. K.; Meyer, T. J.; *Inorg. Chem.* **2005**, *44*, 6802-6827.

(5) Dau, H.; Limberg, C.; Reier, T.; Risch, M.; Roggan, S.; Strasser, P. *ChemCatChem* **2010**, *2*, 724-761.

(6) Inoue, H.; Shimada, T.; Kou, Y.; Nabetani, Y.; Masui, D.; Takagi, S.; Tachibana, H. *ChemSusChem* **2011**, *4*, 173-179.

(7) Lichterman, M. F.; Carim, A. I.; McDowell, M. T.; Hu, S.; Gray, H. B.; Brunschwig, B. S.; Lewis, N. S.; *Energy Environ. Sci.* **2014**, *7*, 3334-3337.

(8) Wiechen, M.; Najafpour, M. M.; Allakhverdiev, S. I.; Spiccia, L. *Energy Environ. Sci.* **2014**, *7*, 2203-2212.

(9) Ahn, H. S.; Yano J.; Don Tilley, T. *Energy Environ. Sci.* **2013**, *6*, 3080-3087.

(10) Deng, X.; Tüysüz, H. *ACS Catal.* **2014**, *4*, 3701-3714.

(11) Ruettinger, W.; Dismukes, G. C. *Chem. Rev.* **1997**, *97*, 1-24.

(12) Yagi M.; Kaneko, M. *Chem. Rev.* **2001**, *101*, 21-36.

(13) Limburg, B.; Bouwman, E.; Bonnet, S. *Coord. Chem. Rev.* **2012**, *256*, 1451-1467.

(14) Hetterscheid, D. G. H.; Reek, J. N. H.; *Angew. Chem. Int. Ed.* **2012**, *51*, 9740-9747.

(15) Jiao, F.; Frei, H. *Energy Environ. Sci.*, **2010** *3*, 1018-1027.

(16) Hansen, R. E.; Das, S. *Energy Environ. Sci.* **2014**, *7*, 317-322.

(17) Song, F.; Ding, Y.; Ma, B.; Wang, C.; Wang, Q.; Du, X.; Fu, S.; Song, J. *Energy Environ. Sci.* **2013**, *6*, 1170-1184.

(18) Leung, C.-F.; Ng, S.-M.; Ko, C.-C.; Man, W.-L.; W.-L. Wu, W.-L.; Chen, L.; Lau, T.-C. *Energy Environ. Sci.* **2012**, *5*, 7903-7907.

(19) Yagi, M.; Syouji, A.; Yamada, S.; Komi, M.; Yamazak, H.; Tajima, S. *Photochem. Photobiol. Sci.* **2009**, *8*, 139-147.

(20) Wasylenko, D. J.; Palmer, R. D.; Berlinguette, C. P. *Chem. Commun.* **2013**, *49*, 218-227.

(21) Cao, R.; Lai, W.; Du, P. *Energy Environ. Sci.* **2012**, *5*, 8134-8157.

(22) Liu, X.; Wang, F. *Coord. Chem. Rev.* **2012**, *256*, 1115-1136.

(23) For a comparison between homogeneous and heterogeneous water oxidation catalysts see: Fukuzumi, S.; Hong, D. *Eur. J. Inorg. Chem.* **2014**, 645-659. Vickers, J. W.; Lv, H.; Sumliner, J. M.; Zhu, G.; Luo, Z.; Musaev, D. G.; Geletii, Y. V.; Hill, C. L. *J. Am. Chem. Soc.* **2013**, 135, 14110-14118. Stracke, J. J.; Finke, R. G. *ACS Catal.* **2014**, 4, 909-933.

(24) (a) Grotjahn, D. B.; Brown, D. B.; Martin, J. K.; Marelius, D. C.; Abadjian, M.-C.; Tran, H. N.; Kalyuzhny, G.; Vecchio, K. S.; Specht, Z. G.; Cortes-Llamas, S. A.; Miranda-Soto, V.; van Niekerk, C.; Moore, C. E.; Rheingold, A. L. *J. Am. Chem. Soc.* **2011**, *133*, 19024-19027. (b) Zuccaccia, C.; Bellachioma, G.; Bolaño S.; Rocchigiani, L.; Savini A.; Macchioni, A. *Eur. J. Inorg. Chem.* **2012**, *1462-1468*. (c) Wang, C.; Wang, J.-L.; Lin, W. *J. Am. Chem. Soc.* **2012**, *134*, 19895-19908. (d) Zuccaccia, C.; Bellachioma, G.; Bortolini, O.; Bucci, A.; Savini A.; Macchioni, A. *Chem.- Eur. J.* **2014**, *20*, 3446-3456. (e) Zhang, T.; de Krafft, K. E.; Wang, J.-L.; Wang, C.; Lin, W. *Eur. J. Inorg. Chem.* **2014**, *4*, 698-707.

(25) Young, K. J.; Martini, L. A.; Milot, R. L.; Snoeberger III, R. C.; Batista, V. S.; Schmuttenmaer, C. A.; Crabtree R. H.; Brudvig, G. W. *Coord. Chem. Rev.* **2012**, *256*, 2503-2520.

(26) Berardi, S.; La Ganga, G.; Puntoriero, F.; Sartorel, A.; Campagna S.; Bonchio, M. *Photochemistry* **2012**, *40*, 274-294.

(27) Brimblecombe, R.; Dismukes, G. C.; Swiegers, G. F.; Spiccia, L. *Dalton Trans.* **2009**, *9374-9384*.

(28) Duan, L.; Tong, L.; Xu Y.; Sun, L. *Energy Environ. Sci.* **2011**, *4*, 3296-3313.

(29) Moore, G. F.; Blakemore, J. D.; Milot, R. L.; Hull, J. F.; Song, H.-E.; Cai, L.; Schmuttenmaer, C. A.; Crabtree, R. H.; Brudvig, G. W. *Energy Environ. Sci.* **2011**, *4*, 2389-2392.

(30) Lin, L.; Duan, L.; Xu, Y.; Gorlov, M.; Hagfeldt, A.; Sun, L. *Chem. Commun.* **2010**, *46*, 7307-7309.

(31) Honda K.; Fujishima, A. *Nature* **1972**, *238*, 37-38.

(32) Grätzel, M. *Nature* **2001**, *414*, 338-344.

(33) Waterhouse, G. I. N.; Wahab, A. K.; Al-Oufi, M.; Jovic, V.; Sun-Waterhouse, D.; Dalaver, A.; Llorca, J.; Idriss, H. *Scientific Reports* **2013**, *3*, 2849, 1-5.

(34) Connelly, K. A.; Idriss, H. *Green Chemistry* **2012**, *14*, 260-280.

(35) Liu, F.; Cardolaccia, T.; Hornstein, B. J.; Schoonover, J. R.; Meyer, T. J. *J. Am. Chem. Soc.* **2007**, *129*, 2446-2447.

(36) Chen, Z.; Conception, J. J.; Jurss, J. W.; Meyer, T. J. *J. Am. Chem. Soc.* **2009**, *131*, 15580-15581.

(37) Francàs, L.; Sala, X.; Benet-Buchholz, J.; Escriche, L.; Llobet, A. *ChemSusChem* **2009**, *2*, 321-329.

(38) McDaniel, N. D.; Coughlin, F. J.; Tinker, L. L.; Bernhard, S. *J. Am. Chem. Soc.* **2008**, *130*, 210-217.

(39) Hull, J. F.; Balcells, D.; Blakemore, J. D.; Incarvito, C. D.; Eisenstein, O.; Brudvig, G. W.; Crebtree, R. H. *J. Am. Chem. Soc.* **2009**, *131*, 8730-8731.

(40) Savini, A.; Bellachioma, G.; Ciancaleoni, G.; Zuccaccia, C.; Zuccaccia, D.; Macchioni, A. *Chem. Commun.* **2010**, *46*, 9218-9219.

(41) Savini, A.; Belanzoni, P.; Bellachioma, G.; Zuccaccia, C.; Zuccaccia, D.; Macchioni, A. *Green Chemistry* **2011**, *13*, 3360-3374.

(42) Savini, A.; Bellachioma, G.; Bolaño, S.; Rocchigiani, L.; Zuccaccia, C.; Zuccaccia, C.; Zuccaccia, D.; Macchioni, A. *ChemSusChem* **2012**, *5*, 1415-1419.

(43) Bucci, A.; Savini, A.; Rocchigiani, L.; Zuccaccia, C.; Rizzato, S.; Albinati, A.; Llobet, A.; Macchioni, A. *Organometallics* **2012**, *31*, 8071-8074.

(44) Savini, A.; Bucci, A.; Bellachioma, G.; Giancola, S.; Palomba, F.; Rocchigiani, L.; Rossi, A.; Suriani, M.; Zuccaccia, C.; Macchioni, A. *J. Organomet. Chem.* **2014**, 771, 24-32.

(45) Blakemore, J. D.; Schley, N. D.; Balcells, D.; Hull, J. F.; Olack, G. W.; Incarvito, C.; Eisenstein, O.; Brudvig, G. W.; Crebtree, R. H. *J. Am. Chem. Soc.* **2010**, *132*, 16017-16029.

(46) Lalrempuia, R.; McDaniel, N. D.; Mueller-Bunz, H.; Bernhard, S.; Albrecht, M. *Angew. Chem. Int. Ed.* **2010**, *49*, 9765-9768.

(47) Hetterscheid, D. G. H.; Reek, J. N. H. *Chem. Commun.* **2011**, *47*, 2712-2714.

(48) Dzik, W. I.; Calvo, S. E.; Reek, J. N. H.; Lutz, M.; Ciriano, M. A.; Tejel, C.; Hetterscheid, D. G. H.; de Bruin, B. *Organometallics* **2011**, *30*, 372-374.

(49) Marquet, N.; Gärtner, F.; Losse, S.; Pohl, M.-M.; Junge, H.; Beller, M. *ChemSusChem* **2011**, *4*, 1598-1600.

(50) Petronilho, A.; Rahman, M.; Woods, J. A.; Al-Sayyed, H.; Muller-Bunz, H.; Don, M. J. M.; Bernhard, S.; Albrecht, M. *Dalton Trans.* **2012**, *41*, 13074-13080.

(51) Codalà, Z.; Cardoso, J. M. S.; Royo, B.; Costa, M.; Fillol, J. L. *Chem. - Eur. J.* **2013**, *19*, 7203-7213.

(52) Petronilho, A.; Woods, J. A.; Bernhard, S.; Albrecht, M. *Eur. J. Inorg. Chem.* **2014**, *4*, 708-714.

(53) Hong, D.; Murakami, M.; Yamada, Y.; Fukuzumi, S. *Energy Environ. Sci.*, **2012** *5*, 5708-5716.

(54) Woods, J. A.; Lalrempuia, R.; Petronilho, A.; McDaniel, N. D.; Müller-Bunz, H.; Albrecht, M.; Bernhard, S. *Energy Environ. Sci.* **2014**, *7*, 2316-2328.

(55) Guo, Q.; Cocks, I.; Williams, E. M. *Surf. Sci.* **1997**, *393*, 1-11.

(56) Guo, Q.; Williams, E. M. *Surf. Sci.* **1999**, *433–435*, 322-326.

(57) Qiu, T.; M. A. Barteau, *J. Colloid Interface Sci.* **2006**, *303*, *229-235*.

(58) Cocks, D.; Guo, Q.; Williams, E. M. *Surf. Sci* **1997**, *390*, 119-125.

(59) Mattsson, A.; Hu, S.; Hermansson, K.; Österlund, L. *J. Chem. Phys.* **2014**, *140*, 034705.

(60) Gutiérrez-Sosa, A.; Martinéz-Escolano, P.; Raza, H.; Lindsay, R.; Wincott, P. L.; Thornton, G. *Surf. Sci.* **2001**, *471*, 163-169.

(61) Sayago, D. I.; Polcik, M.; Lindsay, R.; Toomes, R. L.; Hoeft, J. T.; Kittel, M.; Woodruff, D. P. *J. Phys. Chem. B* **2004**, *108*, 14316-14323.

(62) Lerotholi, T. J.; Kröger, E. A.; Knight, M. J.; Unterberger, W.; Hogan, K.; Jackson, D. C.; Lamont, C. L. A.; Woodruff, D. P. *Surf. Sci.* **2009**, *603*, 2305-2311.

(63) Muir, J. M. R.; Costa, D.; Idriss, H. *Surf. Sci.* **2014**, *624*, 8-14.

(64) Muir, J.; Idriss, H. *Surf. Sci.* **2013**, *617*, 60-67.

(65) Muir, J.; Idriss, H. *Surf. Sci.* **2013**, *607*, 187-196.

(66) A control experiment using TiO_2 instead of **1**_TiO_2 led to negligible production of oxygen (Figure S1). Such a blank experiment was performed in ambient light waiting one hour before adding CAN. No gas was evolved. Consequently, all experiments were performed in ambient light.

(67) Apparent O_2 yield is less than 100% (Table 1) likely due to some oxygen dissolved in water that is not correctly taken into account by manometric measurements.

(68) Savini, A.; Bucci, A.; Bellachioma, G.; Rocchigiani, L.; Zuccaccia, C.; Llobet, A.; Macchioni, A. *Eur. J. Inorg. Chem.* **2014**, *4*, 690-697.

(69) Bozoglian, F.; Romain, S.; Ertem, M. Z.; Todorova, T. K.; Sens, C.; Mola, J.; Rodríguez, M.; Romero, I.; Benet-Buchholz, J.; Fontrodona, X.; Cramer, C. J.; Gagliardi, L.; Llobet, A. *J. Am. Chem. Soc.* **2009**, *131*, 15176-15187.

(70) Kono, S.; Shiraishi, M.; Plusnin, N. I.; Goto, T.; Ikejima, Y.; Abukawa, T.; Shimomura, M.; Dai, Z.; Bednarski-Meinke C.; Goldi, B. *Diam. Relat. Mater.* **2007**, *16*, 594-599.

(71) Crotti, C.; Farnetti, E.; Filipuzzi, S.; Stener, M.; Zangrandoc, E.; Morasa, P. *Dalton Trans.* **2007**, 133-142.

(72) Idriss, H.; Barteau, M. A. *Adv. Catal.* **2000**, *45*, 261-331

(73) Saito, M.; Uehiro, T.; Yoshino, Y.; *Bull. Chem. Soc. Jpn.* **1980**, *53*, 3531-3536.

- FOR TABLE OF CONTENTS USE ONLY -

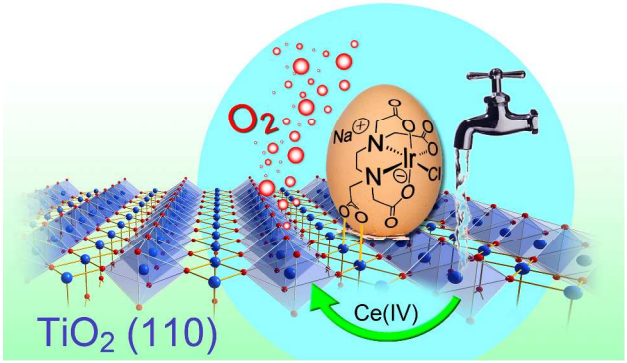

The simple molecular water oxidation catalyst, [Ir(Hedta)Cl]Na (*egg of Columbus*), was successfully immobilized onto rutile-TiO_2 (*tap the egg gently on the table*) leading to an extremely active heterogenized catalyst with performances higher than those of its molecular precursor.